Available online at www.sciencedirect.com
SCIENCE DIRECT®
Journal of Solid State Chemistry 179 (2006) 315–322
JOURNAL OF SOLID STATE CHEMISTRY
www.elsevier.com/locate/jssc

The reciprocal $CuInS_2 + 2CdSe \Leftrightarrow CuInSe_2 + 2CdS$ system. Part I. The quasi-binary $CuInSe_2$–CdSe system: Phase diagram and crystal structure of solid solutions

I.D. Olekseyuk, O.V. Parasyuk*, O.A. Dzham, L.V. Piskach

Department of General and Inorganic Chemistry, Volyn State University, Voli Avenue 13, Lutsk 43009, Ukraine

Received 18 June 2004; received in revised form 21 September 2005; accepted 23 September 2005
Available online 4 November 2005

Abstract

The type of interaction in quasi-binary system $CuInSe_2$ (CIS)–CdSe was investigated using differential thermal and X-ray phase analysis methods. The limits of existence of solid solutions based on low-temperature (α) and high-temperature (γ) CIS modifications and CdSe (β) with chalcopyrite, sphalerite and wurtzite structures, respectively, were established in sub-solidus region at 620 K and 870 K. For certain compositions of solid solutions, the structure was refined using powder X-ray diffraction. A phase diagram of the CIS–CdSe system was constructed. A peritectic process $L + \beta \Leftrightarrow \gamma$ takes place in the system at 1260 K.

Keywords: Semiconductors; Liquid–solid reaction; Phase diagrams; Thermal analysis

1. Introduction

The interest in $CuIn(Ga)S(Se,Te)_2$ compounds and their solid solutions rose in recent years due to their prospective use as material in absorption layer of solar cells. The highest interest is in $CuInSe_2$ compound (CIS) [1]. Photovoltaic solar elements based on CIS have a conversion coefficient of 18% [2] and are commercially relevant on their price/efficiency ratio. CIS bandgap equals, according to various authors, 0.96–1.1 eV [3], i.e. it lies at the boundary of the solar radiation spectrum. Solid solutions of CIS–$CuGaSe_2$ and CIS–$CuInS_2$ systems are used to increase the bandgap and conversion efficiency. In $CuIn_{1-x}Ga_xSe_2$ ($0 \leqslant x \leqslant 0.3$) (CIGS) solid solutions the bandgap increases to 1.2 eV. Their use led to an increase of the conversion coefficient to 20–21% [4]. Further increase of $CuGaSe_2$ content in CIGS, though leading to the increase in bandgap, decreases the conversion coefficient [5]. One of the ways of decreasing the cost of solar batteries is full or partial substitution of In by a less expensive element. Full substitution ($2In \rightarrow A^{II} + B^{IV}$), as was shown in the Cu_2ZnSnS_4 example [6–8], significantly decreases the conversion efficiency (2.62%) [7]. It must be noted, however, that the family of compounds with the stannine structure has a number of representatives that may be used as CIS substitutes based on their initial parameters [9,10] but have not yet been investigated in this role. Partial indium substitution will perhaps be more advantageous. For instance, large regions of solid solutions that are perspective in solar radiation photoconversion [14] form in the CIS–ZnSe system [11–14]. An analogous system with CdSe is also of high interest. There, the formation of a quaternary intermediate phase with a wide homogeneity region based on $CuCd_2InSe_4$ composition is known [15–17], that is photosensitive [16], has 1.1–1.3 eV bandgap [15] and like CIS, may be obtained with both *p*- [16] and *n*- [15] conductivity types. CIS–CdSe system was earlier investigated in Refs. [15,16]. Common in both papers is the existence of an intermediate phase with a wide homogeneity region that crystallizes in the sphalerite structure. However, in Ref. [15] the authors present it as

*Corresponding author. Fax: +7 380 332 241 007.
E-mail address: oleg@lab.univer.lutsk.ua (O.V. Parasyuk).

0022-4596/$ - see front matter © 2005 Elsevier Inc. All rights reserved.
doi:10.1016/j.jssc.2005.09.035

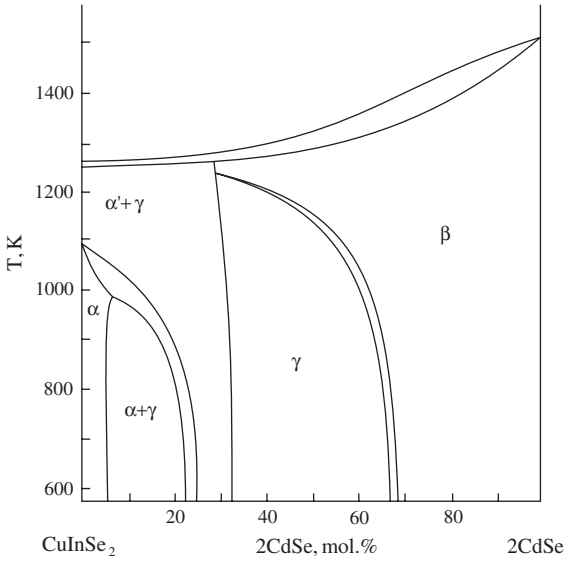

Fig. 1. Phase diagram of the $CuInSe_2$–2CdSe system [15].

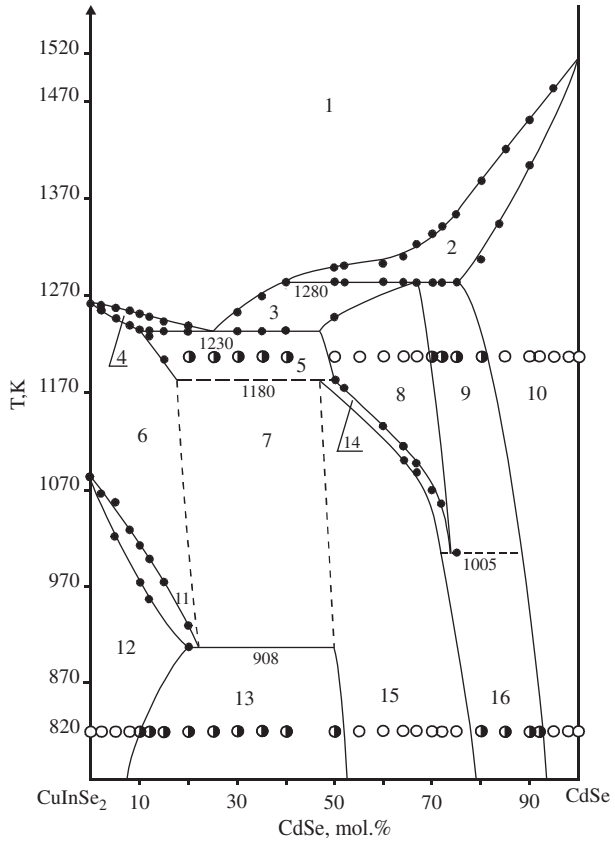

Fig. 2. Phase diagram of the $CuInSe_2$–CdSe system [16]: 1, L; 2, L + CdSe(β); 3, L + $CuCd_2InSe_4$(η); 4, L + $CuInSe_2$(ε); 5, $\varepsilon+\eta$; 6, ε; 7, $\varepsilon+\gamma$; 8, η; 9, $\eta+\beta$; 10, β; 11, $\varepsilon+\alpha$; 12, α; 13, $\alpha+\gamma$; 14, $\eta+\gamma$; 15, γ; 16, $\gamma+\beta$.

a solid-state compound (Fig. 1), whereas in Ref. [16] it forms via a peritectic reaction (Fig. 2). The constructed diagrams also have other significant differences.

Garbato et al. [15] established three single-phase fields: with tetragonal structure (α-solid solution based on a low-temperature (LT) CIS modification), with cubic structure (γ-solid solution), and with hexagonal structure (β-solid solution based on CdSe), that lie in $0 \leqslant x \leqslant 5$ mol% 2CdSe, $33 \leqslant x < 67$ mol% 2CdSe and $69 < x \leqslant 100$ mol% 2CdSe ranges, respectively. However, the authors have not interpreted a phase field that lies between the $\alpha+\beta$ and $\alpha'+\beta$ fields. The co-existence of the two-phase field $\alpha'+\beta$ and the single-phase γ at near-solidus temperatures is also unlikely. Some fundamental properties of alloys in the system were determined. The alloys of γ-phase have n-type conductivity. The bandgap in the homogeneity region increases with CdSe content from 1.1 to 1.3 eV.

The phase diagram constructed in Ref. [16] is shown in Fig. 2. Eutectic point coordinates are 25 mol% CdSe and 1230 K. A quaternary-phase $CuCd_2InSe_4$ that melts incongruently exists in the system. Peritectic point coordinates are 40 mol% CdSe and 1280 K. Quaternary phase has a polymorphic transformation with its temperature decreasing from 1180 to 1005 K with the increase of cadmium selenide content. At the annealing temperature (820 K), three single-phase regions were discovered: in 0–10 mol% CdSe range (0–~5.3 mol% 2CdSe) with the chalcopyrite structure, 52–78 mol% CdSe range (~35–~56.3 mol% 2CdSe) with the sphalerite structure and 92.5–100 mol% CdSe range (~86–100 mol% 2CdSe) with the wurtzite structure. $CuCd_2InSe_4$ phase exhibits p-type conductivity and is photosensitive. A peculiarity of spectral distribution of photoconductivity is the existence of two maxima that correspond to energies of 1.1 and 1.65 eV.

Significant difference in phase diagrams of the CIS–CdSe system presented in Figs. 1 and 2, caused the necessity of its reinvestigation. This necessity is further aggravated by the fact that both $CuCd_2InSe_4$ phase and high-temperature (HT) CIS modification crystallize in the sphalerite structure. Therefore, an assumption that the quaternary phase is a stabilized to the annealing temperature solid solution based on HT CIS modification is quite plausible.

2. Experimental

Two series of alloys were prepared to establish phase equlibria in CIS–CdSe system. They were synthesized under the same conditions differing only in the annealing temperatures that equalled 870 K for one series and 620 K for another. The alloys were synthesized from high-purity Cu (99.99 wt%), Cd (99.9999 wt%), In (99.99 wt%) and Se (99.997 wt%). The calculated amounts of elements were placed in quartz ampoules, which were evacuated and soldered. The ampoules were then placed in a vertical furnace and heated at a rate of 40–50 K/h to 1420 K. They were retained at that temperature for 6 h with periodic vibration and then cooled to the annealing temperature at a rate of 10 K/h. Alloys were annealed at 870 K for 500 h and at 620 K for 1440 h. The preparation process was

completed by quenching the ampoules with alloys in cold water. Obtained alloys were investigated using differential thermal (Paulik-Paulik-Erdey derivatograph with Pt/Pt–Rh thermocouple) and X-ray diffraction (DRON 4-13 diffractometer with CuK_α-radiation) analyses.

The calculation of lattice parameters and the refinement of crystal structure of certain alloys from solid solution regions were performed using the CSD program package [18].

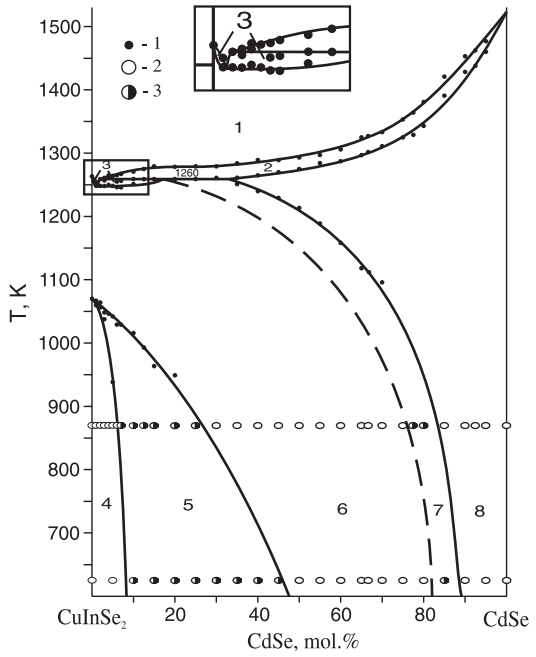

Fig. 3. Phase diagram of the $CuInSe_2$–CdSe system (point labels: 1, DTA results; 2, single-phase alloys; 3, two-phase alloys; fields labels: 1, L; 2, $L+\beta$; 3, $L+\gamma$; 4, α; 5, $\gamma+\alpha$; 6, γ; 7, $\beta+\gamma$; 8, β).

3. Phase diagram of the $CuInSe_2$–CdSe system and crystal structure refinement of the $Cu_{0.97}Cd_{0.06}In_{0.97}Se_2$, $Cu_{1.5}CdIn_{1.5}Se_4$, $Cu_{0.93}Cd_{2.15}In_{0.93}Se_4$ and $Cu_{0.09}Cd_{0.82}In_{0.09}Se$ phases

Based on obtained results, a diagram of phase equlibria in the CIS–CdSe system was constructed. It is presented in Fig. 3. The thermograms of certain alloys of the system are shown in Fig. 4. A peritectic process $L+\beta \Leftrightarrow \gamma$ takes place in the system (non-variant point coordinates are 2 mol% CdSe and 1260 K). The position of liquidus and solidus lines agrees well with results in Ref. [15]. We did not observe the formation of eutectic suggested in Ref. [16]. In the region near CIS, the curve of the solid solution crystallization exhibits a minimum. The point at which liquidus and solidus lines converge is between 1 and 2 mol% CdSe.

Typical diffraction patterns of alloys annealed at 870 and 620 K are shown in Figs. 5 and 6, respectively. Three sets of diffraction reflections that correspond to tetragonal

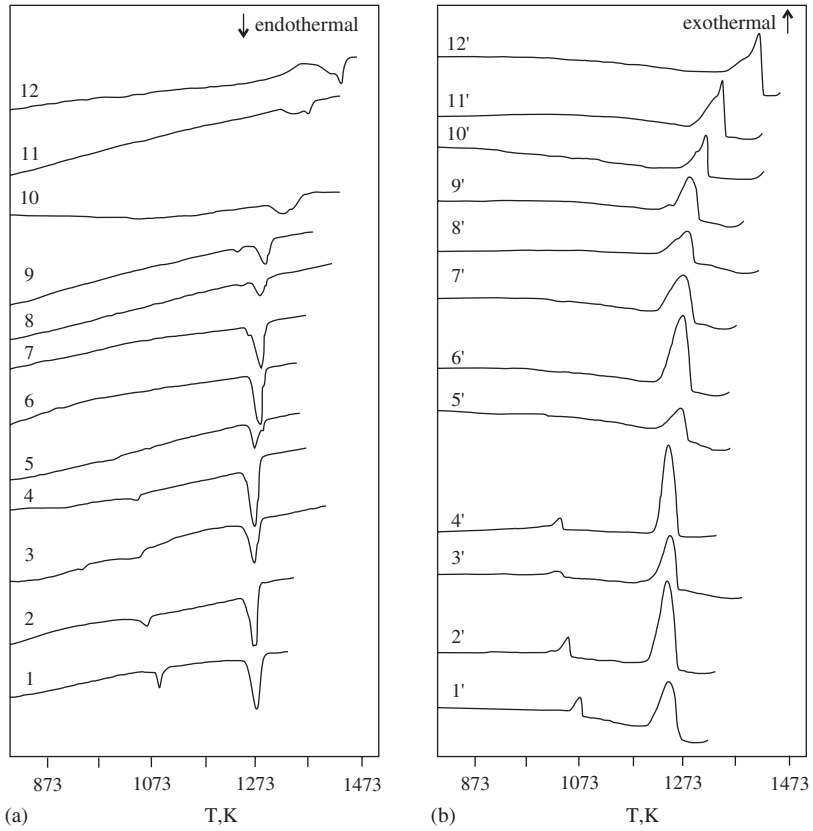

Fig. 4. Heating (a) and cooling (b) thermograms of the $CuInSe_2$–CdSe system alloys (all in mol% CdSe): (1,1′) 0; (2,2′) 3; (3,3′) 5; (4,4′) 7; (5,5′) 12.5; (6,6′) 25; (7,7′) 35; (8,8′) 40, (9,9′) 45; (10,10′) 66.7; (11,11′) 75; (12,12′) 85.

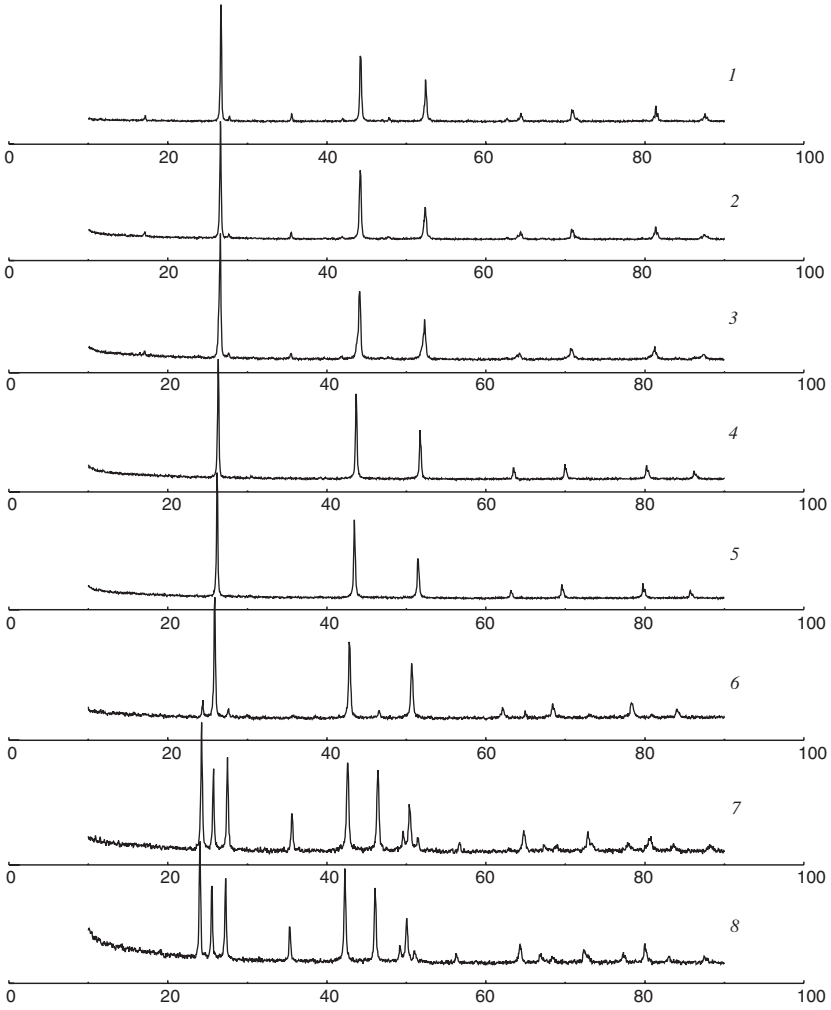

Fig. 5. XRD patterns of samples of the $CuInSe_2$–CdSe system annealed at 870 K (all in mol% CdSe): (1) 0; (2) 5; (3) 15; (4) 35; (5) 50; (6) 80; (7) 85; (8) 100.

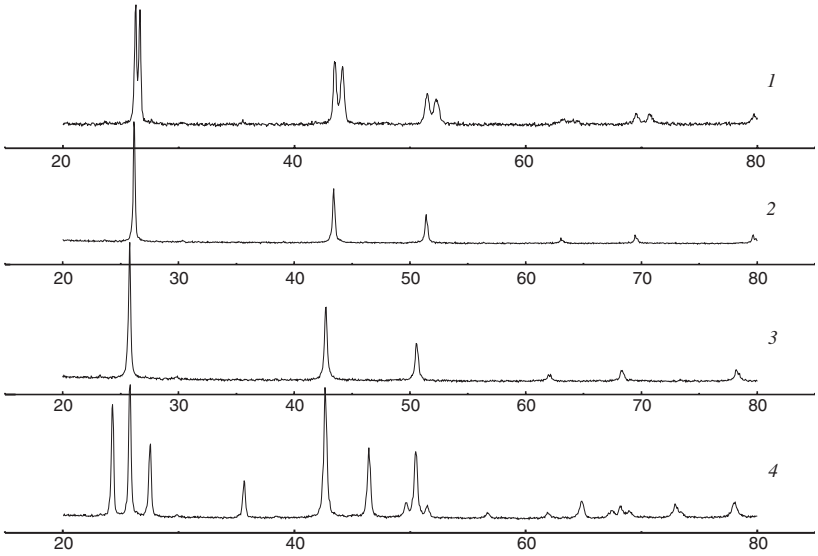

Fig. 6. XRD patterns of samples of the $CuInSe_2$–CdSe system annealed at 620 K (all in mol% CdSe): (1) 35, (2) 50, (3) 80, (4) 85.

and cubic CIS modifications, hexagonal CdSe, or their combination can be seen on the alloy diffraction patterns. For instance, diffraction patterns (*1,2*) in Fig. 5 contain sets of peaks typical of the chalcopyrite structure whereas patterns (*4,5*) contain peaks that belong to the sphalerite structure. Pattern (*3*) exhibits a mix of both structures, which was confirmed by the profile analysis. In Fig. 6, the diffraction pattern of the alloy with 35 mol% CdSe (*1*) illustrates the same picture more clearly, which is caused by the decrease of region of solid solution with cubic structure (see also diffraction pattern (*4*) in Fig. 5) and, consequently, a greater 2Θ shift of the peaks. Alloys with 50 mol% CdSe is single phase at both 870 K ((*5*), Fig. 5) and 620 K ((*2*), Fig. 6). The presented diffraction patterns reveal a significant difference between the results of this work (especially at higher temperatures) and previous studies [15,16]. This difference may be caused by a delay between the completion of alloys synthesis and their X-ray phase analysis during which partial decomposition of γ-solid solution could occur. The existence of γ-solid solution is established in a rather wide concentration range as evidenced by alloy diffraction patterns as well as the peak shift with varying component concentration and respective change in lattice parameters (Fig. 7). Diffraction patterns of alloys with 80 mol% CdSe are of interest. The sphalerite structure is established only at 620 K ((*3*), Fig. 6) whereas at 870 K a mix of diffraction reflections of sphalerite and wurtzite phases is observed ((*6*), Fig. 5). Meanwhile, an inverse picture is observed for β-solid solutions with the wurtzite structure. The alloy with 85 mol% CdSe ((*7*), Fig. 5) is single-phase at 870 K. Its diffraction pattern corresponds to the hexagonal wurtzite-type structure with notable peak shift compared to CdSe ((*8*), Fig. 5). This same alloy is two-phase at 620 K ((*4*), Fig. 6).

The solubility in β-solid solution reaches a maximum at the peritectic temperature (~33 mol% CdSe) and substantially decreases with temperature decrease. For instance, β-solid solution exists in 84–100 mol% CdSe range at 870 K and in 89–100 mol% CdSe range at 620 K (Fig. 3,7). γ-Solid solution that crystallizes in the sphalerite structure forms in three ways: immediately from the melt (in 0–2 mol% CdSe range), as a product of the peritectic process (2–~33 mol% CdSe) and during the decomposition of β-solid solution. The presence of thermal effects related to the CIS phase transformation and phase analysis of alloys annealed at different temperatures confirm our assumption that the quaternary compound is, in fact, a solid solution based on HT-$CuInSe_2$, stabilized to annealing temperatures by an addition of CdSe. The solubility limits for γ-solid solution determined by concentration change of unit cell periods range from 26 to 76 mol% CdSe at 870 K and from 47 to 83 mol% CdSe at 620 K. α-Solid solution has the chalcopyrite structure and is localized in a concentration range of 0–6 mol% CdSe at 870 K and 0–8 mol% CdSe at 620 K.

The refinement of crystal structure using powder X-ray diffraction was performed for alloys with 6 mol% CdSe (chalcopyrite structure), 40 and 70 mol% CdSe (sphalerite structure), that were annealed at 870 K, and an alloy with 90 mol% CdSe annealed at 620 K. The experimental

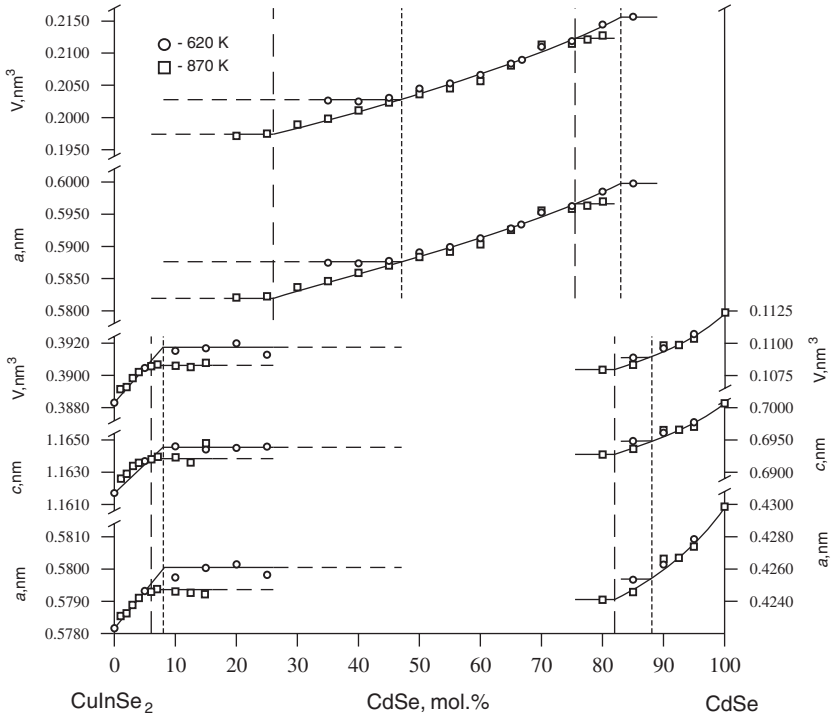

Fig. 7. Plots of lattice parameters and unit cell volumes of the solid solutions in the $CuInSe_2$–CdSe system.

Table 1
Results of the crystal structure determination of the $Cu_{0.97}Cd_{0.06}In_{0.97}Se_2$, $Cu_{1.5}CdIn_{1.5}Se_4$, $Cu_{0.93}Cd_{2.15}In_{0.93}Se_4$ and $Cu_{0.09}Cd_{0.82}In_{0.09}Se$ phases

Compound	$Cu_{0.97}Cd_{0.06}In_{0.97}Se_2$	$Cu_{1.5}CdIn_{1.5}Se_4$	$Cu_{0.93}Cd_{2.15}In_{0.93}Se_4$	$Cu_{0.09}Cd_{0.82}In_{0.09}Se$
Number of formula units per unit cell	4	4	4	4
Space group	$I\bar{4}2d$	$F\bar{4}3m$	$F\bar{4}3m$	$P6_3mc$
a (nm)	0.57931(2)	0.58678(3)	0.59598(4)	0.42613(2)
c (nm)	1.16383(6)	—	—	6.9590(4)
Cell volume (nm^3)	0.39059(4)	0.20204(3)	0.21169(4)	0.10944(2)
Number of atoms in the cell	16.0	8.0	8.0	4.0
Calculated density (g/cm^3)	5.7361(6)	5.7177(9)	5.641(1)	5.6567(8)
Absorption coefficient (1/cm)	785.06	835.77	886.88	943.87
Radiation and wavelength	Cu 0.154178 nm			
Diffractometer	Powder DRON 4-13			
Mode of refinement	Full profile			
Number of atom sites	3	2	2	2
Number of free parameters	6	5	5	6
2Θ and $\sin\Theta/\lambda$ (max)	97.74, 0.489	96.18, 0.483	94.48, 0.476	99.20, 0.494
R_I, R_P	0.0526, 0.0921	0.0480, 0.0642	0.0540, 0.0756	0.0767, 0.1207
Texture axis and parameter	[001] 0.931(7)	[001] 0.6(2)	[001] 2.7(1)	[111] 0.25 (2)

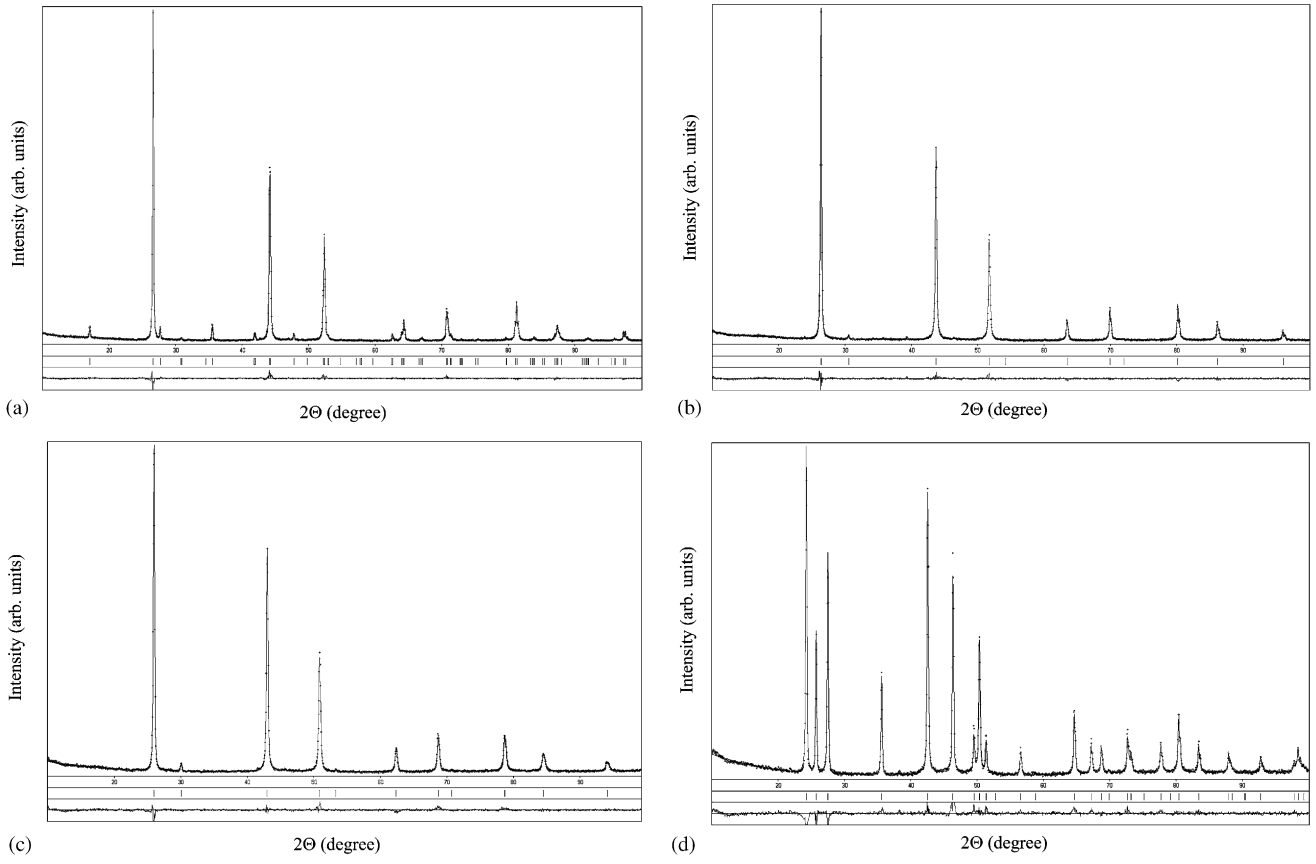

Fig. 8. Experimental and calculated diffractograms and corresponding difference diagram for the $Cu_{0.97}Cd_{0.06}In_{0.97}Se_2$ (a), $Cu_{1.5}CdIn_{1.5}Se_4$ (b), $Cu_{0.93}Cd_{2.15}In_{0.93}Se_4$ (c) and $Cu_{0.09}Cd_{0.82}In_{0.09}Se$ (d) phases.

conditions and crystallographic parameters of the phases are given in Table 1.

It is known [19] that both components of quasi-binary system belong to normal-valent diamond-like compounds and have mixed ion-covalent type of chemical bonding. The crystal structure of such compounds can be described as a closest packing of anion atoms (Se in this case), where half of the tetrahedral void is filled with cation atoms. Such

Table 2
Atomic coordinates and isotropic temperature factors for the $Cu_{0.97}Cd_{0.06}In_{0.97}Se_2$, $Cu_{1.5}CdIn_{1.5}Se_4$, $Cu_{0.93}Cd_{2.15}In_{0.93}Se_4$ and $Cu_{0.09}Cd_{0.82}In_{0.09}Se$ phases

Atom	Position	x/a	y/b	Z/c	$B_{iso} \times 10^2$ (nm^2)
$Cu_{0.97}Cd_{0.06}In_{0.97}Se_2$					
M1[a]	4(*a*)	0	0	0	0.955(8)
M2[b]	4(*b*)	0	0	1/2	0.788(7)
Se1	8(*d*)	0.2260(3)	1/4	1/8	0.623(7)
$Cu_{1.5}CdIn_{1.5}Se_4$					
M3[c]	4(*c*)	0	0	0	1.21(10)
Se1	4(*a*)	1/4	1/4	1/4	1.10(12)
$Cu_{0.93}Cd_{2.15}In_{0.93}Se_4$					
M4[d]	4(*c*)	0	0	0	0.82(7)
Se1	4(*a*)	1/4	1/4	1/4	0.59(8)
$Cu_{0.09}Cd_{0.82}In_{0.09}Se$					
M5[e]	2(*b*)	1/3	2/3	−0.0001(4)	0.72(7)
Se1	2(*b*)	1/3	2/3	0.3776(4)	0.35(10)

[a]M1 = 0.977(6)Cu + 0.023(6)Cd.
[b]M2 = 0.98(3)In + 0.02(3)Cd.
[c]M3 = 0.375(3)Cu + 0.250(3)Cd + 0.375(6)In.
[d]M4 = 0.227(2)Cu + 0.538(3)Cd + 0.226(6)In.
[e]M5 = 0.095(6)Cu + 0.798(3)Cd + 0.102(3)In.

an approach was applied in the present study and the best results of structure computation were obtained for the statistical distribution of metal atoms in cation positions. Experimental and calculated parameters of these diffraction patterns are presented in Fig. 8.

Coordinates and isotropic thermal parameters of compound atoms are given in Table 2, interatomic distances and coordination surrounding of atoms in phase structures are listed in Table 3. All cations have a tetrahedral surrounding formed by selenium atoms. Anion atoms, in turn, are surrounded by cations that form a tetrahedron.

4. Conclusion

As we can see from the presented results, the constructed phase diagram of the $CuInSe_2$ (CIS)–CdSe system differs substantially from that given in Refs. [15,16]. It was established that the phase with cubic structure is, in fact, a solid solution based on HT CIS modification that is stabilized at lower temperatures by an addition of cadmium selenide, and not an intermediate phase, as indicated in previous papers.

The phase with cubic structure exists in a wide concentration range; the increase of bandgap is observed in its limits [15]. The alloys of this region are photosensitive and can be obtained, like CIS, with either p- or n-type conductivity [15,16], which make them perspective materials for solar elements based on $A^{II}B^{VI}$ compounds.

Acknowledgments

This work has been financially supported by the Science and Technology Centre of Ukraine (STCU), Project Gr-91j.

Table 3
Interatomic distances δ (nm) and coordination numbers (CN) of the atoms in the $Cu_{0.97}Cd_{0.06}In_{0.97}Se_2$, $Cu_{1.5}CdIn_{1.5}Se_4$, $Cu_{0.93}Cd_{2.15}In_{0.93}Se_4$ and $Cu_{0.09}Cd_{0.82}In_{0.09}Se$ structures

Atoms	δ (nm)	CN	
$Cu_{0.97}Cd_{0.06}In_{0.97}Se_2$			
M1[a]	−4Se	0.2435(1)	4
M2[b]	−4Se	0.2595(1)	4
Se	−2M1	0.2435(1)	4
	−2M2	0.2595(1)	
$Cu_{1.5}CdIn_{1.5}Se_4$			
M3[c]	−4Se	0.25408(1)	4
Se	−4M3	0.25408(1)	4
$Cu_{0.93}Cd_{2.15}In_{0.93}Se_4$			
M4[d]	−4Se	0.25807(1)	4
Se	−4M4	0.25807(1)	4
$Cu_{0.09}Cd_{0.82}In_{0.09}Se$			
M5[e]	−3Se	0.2603(1)	4
	−1Se	0.2628(4)	
Se	−3M5	0.2603(1)	4
	−1M5	0.2628(4)	

[a]M1 = 0.977(6)Cu + 0.023(6)Cd.
[b]M2 = 0.98(3)In + 0.02(3)Cd.
[c]M3 = 0.375(3)Cu + 0.250(3)Cd + 0.375(6)In.
[d]M4 = 0.227(2)Cu + 0.538(3)Cd + 0.226(6)In.
[e]M5 = 0.095(6)Cu + 0.798(3)Cd + 0.102(3)In.

Appendix A. Supplementary data

Supplementary data associated with this article can be found in the online version at doi:10.1016/j.jssc.2005.09.035.

References

[1] A. Goetzberger, C. Hebling, H.-W. Schock, Mater. Sci. Eng. R 40 (2003) 1.

[2] V.Yu. Rud', Yu.V. Rud', Fiz. Tech. Poluprovodnikov 33 (1999) 801.

[3] V.B. Lazarev, Z.Z. Kish, E.Yu. Peresh, E.E. Semrad, Complex Chalcogenides in A^{I}–B^{III}–C^{VI} Systems, Metallurgiya, Moscow, 1993 (in Russian).

[4] K. Ramanathan, M.A. Contreras, B. Egaas, F.S. Hasoon, R.N. Bhattacharya, R. Noufi, in: ICTMC-12. Proceedings of the 12th International Conference on Ternary and Multinary Compounds, Taiwan, 2000.

[5] V.F. Gremenok, I.V. Bodnar', V.Yu. Rud', Yu.V. Rud', H.-W. Schock, Fiz. Tech. Poluprovodnikov 36 (2002) 360.

[6] N. Nokayama, K. Ito, Appl. Surf. Sci 92 (1996) 171.

[7] H. Katagiri, K. Saitoh, T. Washio, H. Shinohara, T. Kurumadani, S. Miyajima, Sol. Energy Mater. Sol. Cells 65 (2001) 141.

[8] J. Madarasz, P. Bombicz, M. Okuya, S. Kaneko, Solid State Ionics 141–142 (2001) 439.

[9] H. Matsushita, T. Maeda, A. Katsui, T. Takizawa, J. Cryst. Growth 208 (2000) 416.

[10] N.N. Konstantinova, G.A. Medvedkin, I.K. Polushina, Yu.V. Rud', A.D. Smirnova, V.I. Sokolova, M.A. Tairov, Neorg. Mater. 25 (1989) 1445.

[11] I.V. Bodnar', L.V. Chibusova, Zh. Neorg. Khim. 43 (1998) 1913.

[12] V.O. Halka, I.D. Olekseyuk, O.V. Parasyuk, X Sci.-pract. Conference on Complex Oxides, Chalcogenides and Halogenides for Functional Electronics, Abstract, Uzhgorod, 2000, p. 45.

[13] V.V. Lisnyak, N.V. Stus, R.T. Mariychuk, Sol. Energy Mater. Sol. Cells 76 (2003) 553.

[14] I.V. Bodnar', V.F. Gremenok, Neorg. Mater. 39 (2003) 1301.

[15] L. Garbato, F. Ledda, P. Manca, A. Rucci, A. Spiga, Prog. Cryst. Growth Characterization 10 (1985) 199.

[16] P. Vovk, G. Davydyuk, I. Mishchenko, O. Zmiy, Visnyk L'viv Univer 39 (2000) 167.

[17] E. Parthè, K. Yvon, R.H. Deitch, Acta Crystallogr. B 25 (1969) 1164.

[18] L.G. Akselrud, Yu.N. Grin', P.Yu. Zavalij, V.K. Pecharsky, V.S. Fundamensky, Collected Abstracts of the 12th European Crystallographic Meeting, vol. 3, Moscow, August 1989, Izv. Acad. Nauk SSSR, Moscow, 1989, p. 155.

[19] N.A. Goryunova, The Complex Diamond-Structure Semiconductors, Sov. radio, Moscow, 1968 (in Russian).